Experimental report

25/05/2020

Proposal: 7-05-496 **Council:** 10/2018

Title: Elucidating the role of energy dissipation and electronic friction innanoscale diffusion

Research area: Physics

This proposal is a resubmission of 7-05-482

Main proposer: Anton TAMTOEGL

Experimental team: Peter FOUQUET
Anton TAMTOEGL
Emma EHRENREICH PETERSEN
Martin OTTESEN

Local contacts: Peter FOUQUET
Orsolya CZAKKEL
Jean Marc ZANOTTI

Samples: Graphite
s-Triazine (C3H3N3)
Deuterated Pyrazine (C4D4N2)

Instrument	Requested days	Allocated days	From	To
IN6-SHARP	6	0		
IN11	14	4	19/06/2019	23/06/2019

Abstract:

We plan to characterise the effect of van-der-Waals (vdW) interactions between heterocyclic analogues of benzene and graphite on the surface diffusion process. Therefore we propose to measure the diffusion of pyrazine (C4H4N2) and s-triazine (C3H3N3) on exfoliated graphite.

By substituting nitrogen atoms into the ring of aromatic hydrocarbons the electronic density around the carbon atoms of the molecule is reduced, giving rise to a stronger bonding with the substrate via tuning of the vdW interaction. Hence, by systematically changing the interaction strength with the substrate, these experiments will allows us to elucidate different aspects of energy dissipation in surface diffusion, in particular the contribution of electronic friction.

Elucidating the role of energy dissipation and electronic friction in nanoscale diffusion (7-05-496 and TEST-2975/2976)

Anton Tamtögl,*,† Marco Sacchi,‡ Michael M. Koza,¶ and Peter Fouquet¶

†*Institute of Experimental Physics, Graz University of Technology, Graz, Austria*
‡*School of Physical Sciences, The Open University, Walton Hall, Milton Keynes MK7 6AA, United Kingdom*
¶*Institut Laue-Langevin, 71 Avenue des Martyrs, 38000 Grenoble, France*

E-mail: tamtoegl@gmail.com

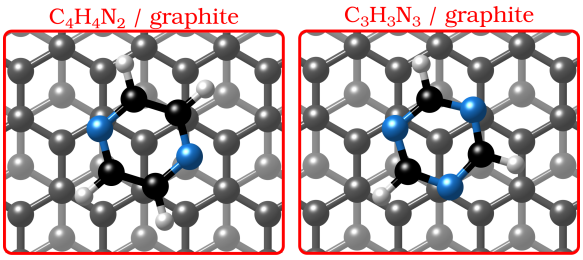

Figure 1: Graphical impression of the heterocyclic organic molecules pyrazine ($C_4H_4N_4$) and s-triazine ($C_3H_3N_3$) adsorbed on graphite.

1 Scientific background

In these experiment we measured the diffusion of pyrazine ($C_4H_4N_2$) and s-triazine ($C_3H_3N_3$) on exfoliated graphite. The project builds upon our long-standing interest in the dynamics of hydrocarbons and small molecules on graphite [1–4]. For benzene (C_6H_6), in particular, we have been able to obtain very detailed spectroscopy data, in recent years [3,4]. By replacing some of the C atoms in benzene (C_6H_6) with N atoms (Figure 1), as done in the described measurements, we are able to compare those with the dynamics of aromatics having similar geometry, but different aromaticity and electronic structure. The introduction of N atoms into the ring reduces the electronic density around the carbon atoms of the molecule and decreases the repulsion between the π-orbitals of the ring and the substrate, giving rise to a stronger bonding to the substrate, because the intensity of the van-der-Waals (vdW) interactions is tuned by the polarisability and electrophilic character of the π-systems of the molecules interacting with the π-system of graphite [5–7].

Benzene adsorbs in a flat (face-face) configuration on graphite and follows Brownian diffusion on this substrate as shown in previous neutron scattering experiments [3,4]. Contrary to benzene, the behaviour of nitrogen containing heterocyclic compounds such as pyrazine ($C_4H_4N_2$) and triazine ($C_3H_3N_3$) on carbon surfaces is much less understood, although previous theoretical studies confirm that, similarly to benzene, these N-containing molecules adsorb with a horizontal configuration at a distance of $3.00-3.21$ Å [5]. Triazine exists in three different isomeric forms and we concentrated our study on the behaviour of the most common and more symmetrical isomer, $1,3,5-$triazine which is also known as s-triazine. S-triazine is essentially as aromatic as benzene, though less polarisable, while pyrazine on the other hand, is slightly less aromatic (85-89%) [8]. Figure 1 shows the structure of both $C_4H_4N_2$ and $C_3H_3N_3$ adsorbed on graphite. Indeed, as shown experimentally, the adsorption geometry of all three molecules on flat metal substrates is in a flat configuration [9–11]. Moreover, scanning tunnelling microscopy (STM) measurements demonstrated that s-triazine adsorbs parallel on highly oriented pyrolytic graphite (HOPG) [10]. Hence, while the adsorption geometry of the molecules remains the same for all three adsorbates, the intensity of the vdW-interactions will be tuned by the number of nitrogen atoms in the ring [5–7].

The adsorption and diffusion of heterocyclic aromatic compounds such as pyrazine and triazine is also interesting for the modification / doping of graphene and graphitic substrates as well as for gas sensing purposes [7,12,13]. It is known that the electronic properties of graphene can be tuned by noncovalent modification via adsorption of heterocyclic aromatic molecules such as pyrazine and triazine. The reversible adsorption of these organic molecules can be used as an effective way to tailor the bandgap structure of graphene (chemical doping of graphene) and it has been shown that the adsorption of molecules such as triazine, pyrazine and borazine on graphene results in a widening of the band gap [7,14]. Hence, the chemical doping of graphene depends strongly on the electrophilic character of the dopants.

2 Experimental details

2.1 Sample preparation

As a substrate we used exfoliated compressed graphite, *Papyex*, which exhibits an effective surface area of about 25 m^2 g^{-1} and retains a sufficiently low defect density [15,16]. Due to its high specific adsorption surface area it is widely used for adsorption measurements. We further exploit the fact that, exfoliated graphite samples exhibit a preferential orientation of the basal plane surfaces and oriented those parallel to the scattering plane of the neutrons. Each sample was prepared with 13-14 g of Papyex exfoliated graphite of grade N998 ($>$ 99.8% C, Carbone Lorraine, Gennevilliers, France). The prepared exfoliated graphite disks were heated to 973 K under vacuum before transferring them into a cylindrical aluminium sample cartridge. The amount of powder $C_3H_3N_3$ and $C_4D_4N_2$, required to reach the corresponding ML coverage, was weighed using a fine balance and then added to the graphite disks. The aluminium sample holders were hermetically sealed using a lid with a steel knife-edge. The samples

were then heated in an evacuated furnace to 423 K to sublimate the powder and promote its adsorption in the whole volume of the sample.

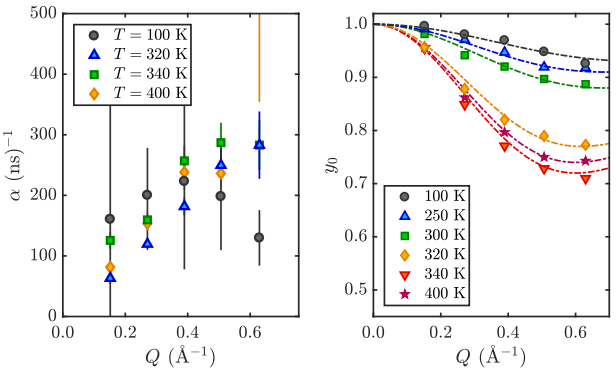

Figure 2: Left panel: Dephasing rate $\alpha = 1/\tau$ versus momentum transfer Q as extracted from the neutron spin-echo measurements for deuterated pyraine ($C_4D_4N_2$) at different temperatures. Right panel: Quasi-elastic amplitude y_0.

2.2 Instrumental details

The measurements were carried out at the IN5 time-of-flight (TOF) neutron spectrometer[17] and the IN11 neutron spin-echo (NSE) spectrometer of the ILL[18,19]. The TOF spectra were converted to scattering functions, $S(Q, \Delta E)$, where $Q = |\mathbf{Q}| = |\mathbf{k_f} - \mathbf{k_i}|$ is the momentum transfer and $\Delta E = E_f - E_i$ is the energy transfer. NSE measurements on the other hand, deliver the development of the space correlation function with time t, i.e., the normalised intermediate scattering function $I(Q,t)/I(Q,0)$[20,21]. The intermediate scattering function is related to the scattering function $S(Q, \Delta E)$ via a Fourier transform in time.

3 Results

Neutron TOF scattering The experimentally measured scattering function $S(Q, \Delta E)$ (normalised by Vanadium) was fitted using a convolution of the resolution function of the neutron TOF spectrometer $S_{res}(Q, \Delta E)$ (scattering function measured at base temperature) with an elastic term $I_{el}(Q)\delta(\Delta E)$, the quasi-elastic contribution $S_{inc}(Q, \Delta E)$ and a linear background:

$$S(Q,\Delta E) = S_{res}(Q,\Delta E) \otimes \left[I_{el}(Q)\delta(\Delta E) + \right. \\ \left. + A(Q)\frac{1}{2\pi}\frac{\Gamma(Q)}{[\Gamma(Q)]^2 + \Delta E^2} + C(Q)\right]. \quad (1)$$

Here, δ represents the Dirac delta and the quasi-elastic broadening is modelled by a Lorentzian function, where $I_{el}(Q)$ is the intensity of the elastic scattering and $A(Q)$ is the intensity of the quasi-elastic scattering. $\Gamma(Q)$ is the half width at half maximum (HWHM) of the Lorentzian.

Neutron spin-echo scattering The intermediate-scattering function (ISF) obtained from the spin-echo measurements was fitted using a stretched exponential decay function (the so-called Kohlrausch Williams Watts function, KWW)

$$I(Q,t) = y_0 + (1 - y_0)\exp\left[-\left(\frac{t}{\tau}\right)^{\beta}\right] \quad (2)$$

where y_0 is the fraction of static signal and β is the stretching exponent ($\beta \leq 1$, with $\beta = 1$ for a single exponential decay).

The NSE measurements were performed for a 0.5 ML sample of $C_4D_4N_2$ adsorbed on exfoliated graphite. Dynamics is already observable starting from low temperatures (100 K) up to 400 K as can be seen from the extracted dephasing rate $\alpha = 1/\tau$ in Figure 2. Upon plotting the the quasi-elastic amplitude y_0 (right panel of Figure 2) it appears that there exist two different dynamical regimes, with the second dynamic process setting in at $T > 300$ K and thus giving rise to larger quasi-elastic amplitude y_0 at higher temperatures. The diffusion of $C_3H_3N_3$ was then measured with neutron TOF, with a first initial test run of 0.5 ML $C_3H_3N_3$ on IN6, followed by a test run of both 0.2 and 0.5 ML $C_3H_3N_3$ on

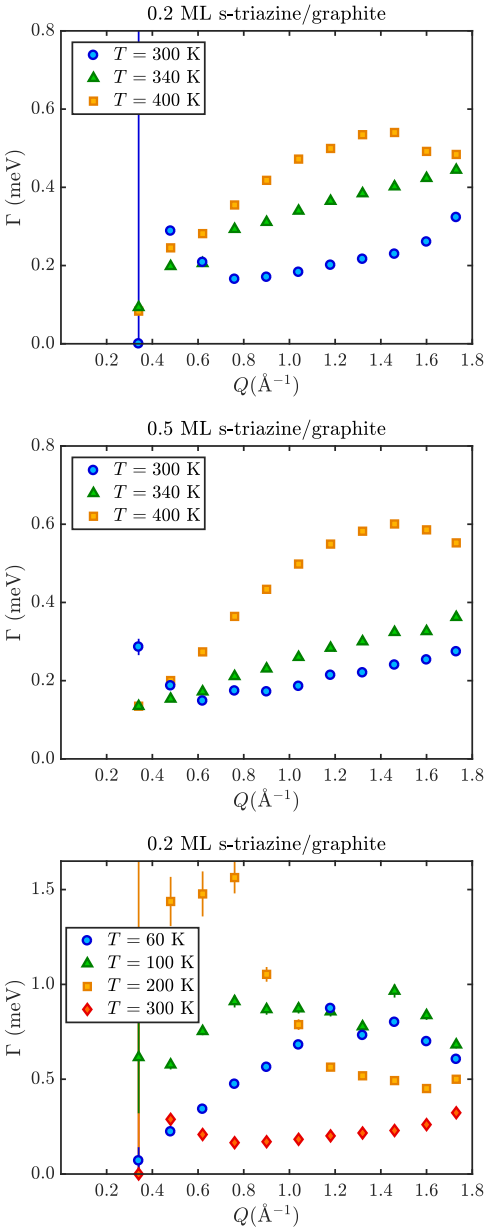

Figure 3: Extracted quasi-elastic broadening $\Gamma(Q)$ for 0.2 and 0.5 ML $C_3H_3N_3$ at several temperatures versus momentum transfer Q.

IN5. Figure 3 shows the extracted quasi-elastic broadenings Γ versus momentum transfer Q upon fitting (1). Again there is evidence fro two dynamic regimes / processes as observed in the NSE data of $C_4D_4N_2$. From the lowest panel in Figure 2 it appears that for the 300 K data Γ is almost constant with respect to Q which could e.g. be due to rotations of the molecule. Further analysis of the experimental data at 60-200 K is required to confirm the reliability/goodness of the fit and in order to provide a thorough analysis of the temperature behaviour. We further note that fitting of the low temperature data also seems to work quite well when using a Gaussian instead of a Lorentzian shape.

From 300 - 400 K (topmost and central panel in Figure 3)

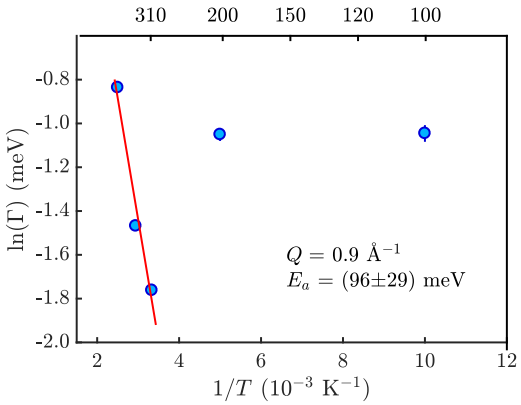

Figure 4: Arrhenius plot for the extracted quasi-elastic broadening $\Gamma(Q)$ for 0.5 ML $C_3H_3N_3$ on graphite.

the broadening shows a much clearer trend in terms of the momentum transfer dependence. The Arrhenius plot (Figure 4), extracted for the measurement at $Q = 0.9$ Å^{-1} illustrates that at about 300 K an activated process seems to set in with an activation energy of about 100 meV.

Thus we conclude from a first preliminary analysis that indeed the substitution of C atoms with N atoms in the benzene ring gives rise to a different diffusive motion. The activated process starting to set in at about 300 K and probably related to the actual mass transport on the surface, appears at much higher temperatures compared to benzene diffusion (Refs.[3,4]). After a more thorough analysis of the experimental data we expect to publish the results together with the vdW corrected DFT calculations in an international peer-reviewed publication.

Acknowledgment

One of us (A.T.) acknowledges financial support provided by the FWF (Austrian Science Fund) within the project P29641-N36. M.S. is grateful for the support from the Royal Society. This work used the ARCHER UK National Supercomputing Service via the membership of the UK's HEC Materials Chemistry Consortium which is funded by the EPSRC (EP/L000202). The authors acknowledge the generous provision of neutron beam time at the ILL[17–19].

References

1. Tamtögl, A.; Sacchi, M. *et al. Carbon* **2018**, *126*, 23–30.
2. Calvo-Almazán, I.; Sacchi, M. *et al. J. Phys. Chem. Lett.* **2016**, *7*, 5285–5290.
3. Calvo-Almazán, I.; Bahn, E. *et al. Carbon* **2014**, *79*, 183 – 191.
4. Hedgeland, H.; Fouquet, P. *et al. Nat Phys* **2009**, *5*, 561–564.
5. Scott, A. M.; Gorb, L. *et al. J. Phys. Chem. C* **2014**, *118*, 4774–4783.
6. Zarudnev, E.; Stepanian, S. *et al. ChemPhysChem* **2016**, *17*, 1204–1212.
7. Zhang, Z.; Huang, H. *et al. The Journal of Physical Chemistry Letters* **2011**, *2*, 2897–2905.
8. Doerksen, R. J.; Steeves, V. J. *et al. Journal of Computational Methods in Sciences and Engineering* **2004**, *4*, 427–438.
9. Wang, D.; Xu, Q.-M. *et al. Langmuir* **2002**, *18*, 5133–5138.
10. Martnez-Galera, A. J.; Gmez-Rodrguez, J. M. *J. Phys. Chem. C* **2011**, *115*, 11089–11094.
11. Dudde, R.; Frank, K.-H. *et al. Journal of electron spectroscopy and related phenomena* **1988**, *47*, 245–255.
12. Cervenka, J.; Budi, A. *et al. Nanoscale* **2015**, *7*, 1471–1478.
13. Tison, Y.; Lagoute, J. *et al. ACS Nano* **2015**, *9*, 670–678.
14. Chang, C.-H.; Fan, X. *et al. J. Phys. Chem. C* **2012**, *116*, 13788–13794.
15. Gilbert, E. P.; Reynolds, P. A. *et al. J. Chem. Soc. Faraday Trans.* **1998**, *94*, 1861–1868.
16. Finkelstein, Y.; Nemirovsky, D. *et al. Physica B Condens Matter* **2000**, *291*, 213 – 218.
17. Tamtögl, A.; Fouquet, P. *et al.* Diffusion of s-triazine on graphite. Institut Laue-Langevin (ILL). doi:10.5291/ILL-DATA.TEST-2975. 2018.
18. Tamtögl, A.; Fouquet, P. Diffusion of deuterated pyrazine on graphite. Institut Laue-Langevin (ILL). doi:10.5291/ILL-DATA.TEST-2976. 2018.
19. Tamtögl, A.; Czakkel, O. *et al.* Elucidating the role of energy dissipation and electronic friction in nanoscale diffusion. Institut Laue-Langevin (ILL). doi:10.5291/ILL-DATA.7-05-496. 2019.
20. Fouquet, P.; Hedgeland, H. *et al. Z. Phys. Chem* **2010**, *224*, 61–81.
21. Mezei, F. In *Neutron Spin Echo: Proceedings of a Laue-Langevin Institut Workshop Grenoble, October 15–16, 1979*; Mezei, F., Ed.; Springer, 1980; Chapter The principles of neutron spin echo, pp 1–26.